

Methods and Applications in Fluorescence



PAPER

Keratin intrinsic fluorescence as a mechanism for non-invasive monitoring of its glycation

OPEN ACCESS

RECEIVED
9 June 2022

REVISED
14 October 2022

ACCEPTED FOR PUBLICATION
22 November 2022

PUBLISHED
1 December 2022

Original content from this work may be used under the terms of the [Creative Commons Attribution 4.0 licence](#).

Any further distribution of this work must maintain attribution to the author(s) and the title of the work, journal citation and DOI.



Rhona Muir¹ , Shareen Forbes², David J S Birch¹ , Vladislav Vyshemirsky³ and Olaf J Rolinski¹

¹ Photophysics Group, Department of Physics, University of Strathclyde, Scottish Universities Physics Alliance, Glasgow G4 0NG, United Kingdom

² BHF Centre for Cardiovascular Science, The Queen's Medical Research Institute, University of Edinburgh, Edinburgh EH16 4TJ, United Kingdom

³ School of Mathematics and Statistics, University of Glasgow, Glasgow G12 8QQ, United Kingdom

E-mail: o.j.rolinski@strath.ac.uk

Keywords: keratin, glucose, protein glycation, intrinsic fluorescence, time-resolved fluorescence spectroscopy

Supplementary material for this article is available [online](#)

Abstract

We have studied the evolution of keratin intrinsic fluorescence as an indicator of its glycation. Steady-state and time-resolved fluorescence of free keratin and keratin-glucose samples were detected in PBS solutions *in vitro*. The changes in the fluorescence response demonstrate that the effect of glucose is manifest in the accelerated formation of fluorescent cross-links with an emission peak at 460 nm and formation of new cross-links with emission peaks at 525 nm and 575 nm. The fluorescence kinetics of these structures is studied and their potential application for the detection of long-term complications of diabetes discussed.

Introduction

Diabetes is characterised by hyperglycaemia. Over time, the increased levels of glucose in the blood can lead to various diabetic complications [1] such as cardiovascular and vascular diseases, stroke, kidney failure, amputation, retinopathy, and neuropathy [2, 3]. Various studies have reported [3, 4] that these complications are related to the presence of glycated proteins. The amount of glycated collagen [5, 6], human serum albumin [7, 8], and haemoglobin [9] have all been found to be increased in patients with diabetes.

Keratin, the protein abundant in hair and nails, can also experience non-enzymatic glycation when exposed to glucose [10–12]. The preferential target for glycation is the ϵ -amino group of a lysine residue or the α -amino group of an N-terminal residue [13, 14], and both sites can be found in keratin. Diabetic patients showed increased levels of glycated keratin in the stratum corneum in the sole of the foot [12], and in hair [10], and in both cases this was detected using the thiobarbituric acid technique. Increased levels of glycated keratin have also been found in fingernails [15–17], using techniques other than fluorescence spectroscopy, which are discussed below. Moreover, a

higher concentration of glycated keratins was found in patients exhibiting complications such as diabetic retinopathy, nephropathy [16], and diabetic ulcers [12], compared to those with diabetes who were not experiencing these complications. These findings therefore suggest that glycated keratin could be a good biomarker for long-term glycaemic control.

Previous studies have used several methods to determine the amount of glycated keratin in human tissues. For example, colorimetric analysis has been used to determine glycated keratin in the stratum corneum of the skin *in vitro* [15], near-infrared reflectance spectroscopy [17], ATR-FTIR spectroscopy [18] and chemical analysis using techniques such as borate affinity chromatography followed by gel electrophoresis [16] has been used to determine the levels of glycated keratin in nail clippings.

In this work, we use fluorescence spectroscopy to detect glycated keratin. Unlike the study in 2015, this method does not require the extraction of nail proteins from a clipping, making it non-destructive for the samples. It also has the capacity to be a non-invasive technique, as we aim to exploit the auto-fluorescence of keratin as a potential method for monitoring its glycation. Being auto-fluorescent, keratin's presence can be detected without the need for any

extrinsic fluorophore. Its fluorescence originates from two sources: amino acids [19] and cross-links within the protein [20, 21].

Keratin contains the naturally fluorescent amino acids phenylalanine (Phe), tyrosine (Tyr), and tryptophan (Trp) [22]. It is however unlikely that Phe will contribute significantly to the intrinsic fluorescence of keratin due to its low absorption and quantum yield [23] and similarly Tyr emission is often reduced in protein by its interaction with the peptide chain or via energy transfer to Trp [24, 25]. Indeed, the amino acid derived fluorescence of keratin peaks at about 340–350 nm [20, 26], which corresponds to Trp fluorescence [24].

The exact number of Trp and Tyr residues in keratin is unknown and differs between specific keratin types. Reports vary, however in α -keratin, which is the type found in mammals, it is thought that Trp and Tyr account for approximately 1% and 3% of the amino acids respectively [22, 27].

Keratin cross-links are the second source of its intrinsic fluorescence. These can be excited at 350–370 nm, and emit fluorescence peaking at \sim 460 nm [20, 28]. These two distinct peaks (Trp and cross-links) have been seen in various keratin-containing tissues such as fingernails, hair, and the stratum corneum [26]. In collagen, which is a similar protein to keratin, glycation causes the formation of new cross-links [29], and it is reasonable to suppose that changes in the fluorescence of the keratin cross-links may offer the most insight into keratin glycation.

If keratin's intrinsic fluorescence changes as a result of glycation, this could provide an alternative method to monitor long-term diabetic control. Keratin is found in human hair, nails, and in the skin, so its fluorescence could in principle be used to monitor diabetes by means, for example, the monitoring of glycated keratin in nail clippings, rather than in blood samples as commonly used at present. This would offer obvious advantage due to the non-invasive nature of the technique. We present this work as a method that is able to more fully investigate the process of keratin glycation, and detect it non-invasively. However, more comprehensive studies would be required to further develop this technique for use in patients, for example to develop a sensor for monitoring long term diabetes control through detecting glycated keratin from nails.

In this work we have studied keratin *in vitro* and have used steady-state and time-resolved fluorescence techniques to investigate the impact of glucose on its intrinsic fluorescence.

Methodology

Sample preparation

The evolution of two samples, free keratin and keratin-glucose, have been studied. Keratin from human epidermis and phosphate buffered saline

pH 7.4 (PBS) were purchased from Sigma-Aldrich and used to prepare a free keratin sample of concentration 20 μ M and the keratin-glucose sample by the addition of glucose powder (also Sigma Aldrich) to create a sample containing 20 μ M keratin and 20 mM glucose. 3.5 ml of each sample was then transferred to a 4x1x1 cm quartz cuvette, and sealed with a stopper and parafilm, ready for measurements. The samples were prepared while maintaining their spectroscopic purity, but were not-sterile, and both samples were stored at room temperature for the duration of the experiment. In the glucose-containing sample, the glycated keratin was not purified from the non-glycated one. To make sure that the spectra measured are not affected by the fluorescence caused by the bacteria growth in the samples, the measurements of a reference sample of glucose in PBS were carried out using the same experimental settings as for the keratin samples. All spectra show that the impact of potential bacteria growth on the keratin and keratin-glucose samples' fluorescence to be negligible (discussed later).

Measurements

Corrected fluorescence excitation and emission spectra were obtained using a Fluorolog (Horiba Scientific). The excitation, emission and the excitation/emission reference samples (discussed later) spectra were collected in steps of 1 nm and the slit widths on the excitation and emission monochromators were 5 nm. The fluorescence intensity decay measurements were carried out on a DeltaFlex fluorescence lifetime system (Horiba Jobin Yvon IBH Ltd, Glasgow), which uses time-correlated single photon counting (TCSPC) to record fluorescence decay. A NanoLED with repetition rate 1MHz and peak excitation wavelength 370 nm (pulse duration $<$ 1 ns) was used for excitation.

The decays measured at each detection wavelength λ were then fitted to the experimental fluorescence curve $I_{exp}(t)$

$$I_{exp}(t) = B + C_{\lambda}(t) + I_{\lambda}(t) \quad (1)$$

which is a combination of the experimental fluorescence intensity decay $I_{\lambda}(t)$ represented by a multi-exponential function

$$I_{\lambda}(t) = \sum_{i=1}^N \alpha_i(\lambda) \exp\left(\frac{-t}{\tau_i(\lambda)}\right) \quad (2)$$

where $\alpha_i(\lambda)$ and $\tau_i(\lambda)$ are the i -th pre-exponential component and its related fluorescence lifetime respectively, B is the background signal, and $C_{\lambda}(t)$ is the scattered excitation light. Including the actual scattered excitation light $C_{\lambda}(t)$ (the fraction of the prompt function shifted in time due to the detecting photomultiplier's temporal dependence on wavelength) into the model of the experimental curve allows accurate fluorescence decay fitting, even when there is a large contribution of scattered light to the decay [30].

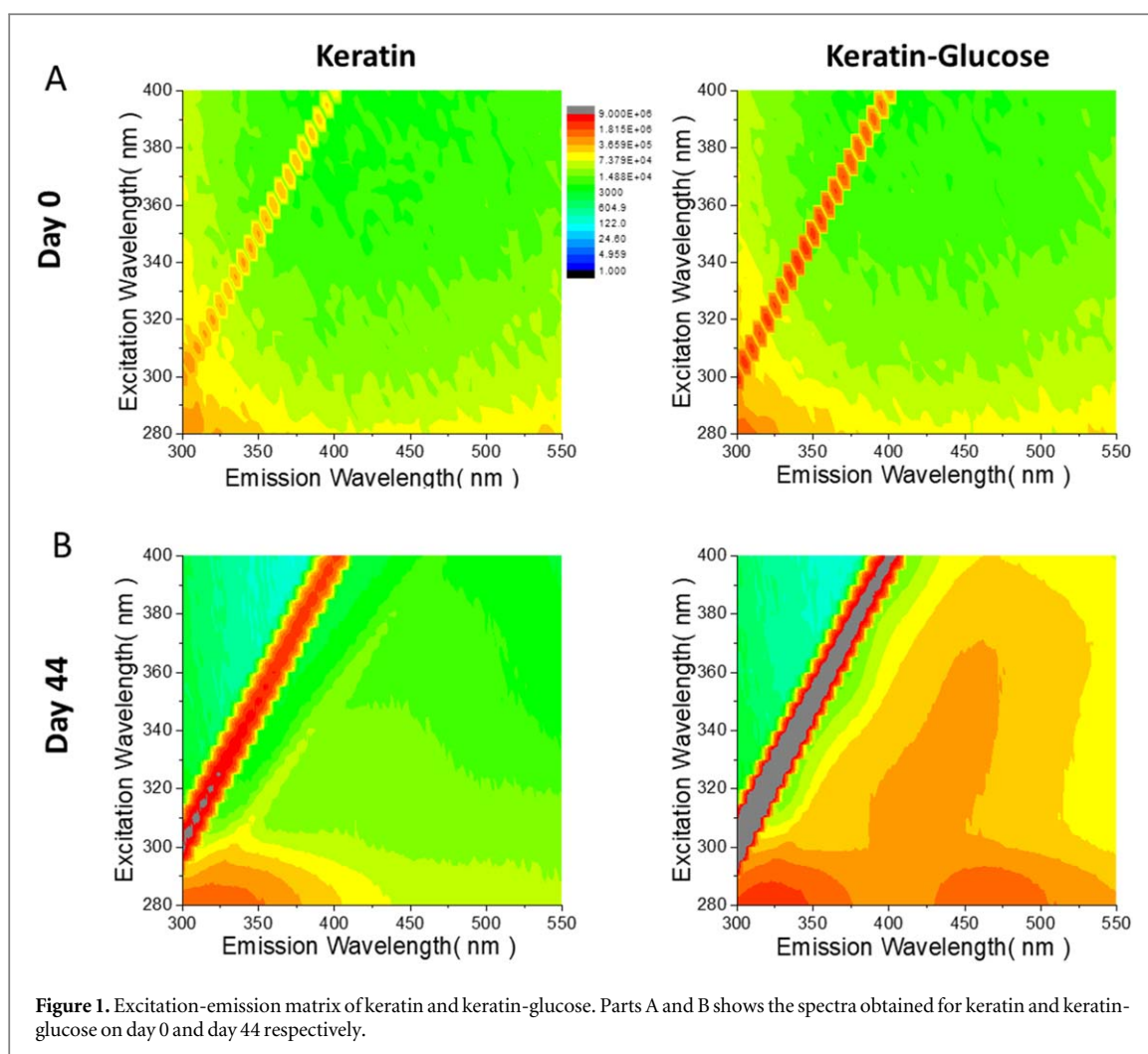


Figure 1. Excitation-emission matrix of keratin and keratin-glucose. Parts A and B shows the spectra obtained for keratin and keratin-glucose on day 0 and day 44 respectively.

The steady state spectra and fluorescence intensity decays were measured for the both samples on day 0 (within ~ 10 min of sample preparation) and on subsequent days after preparation.

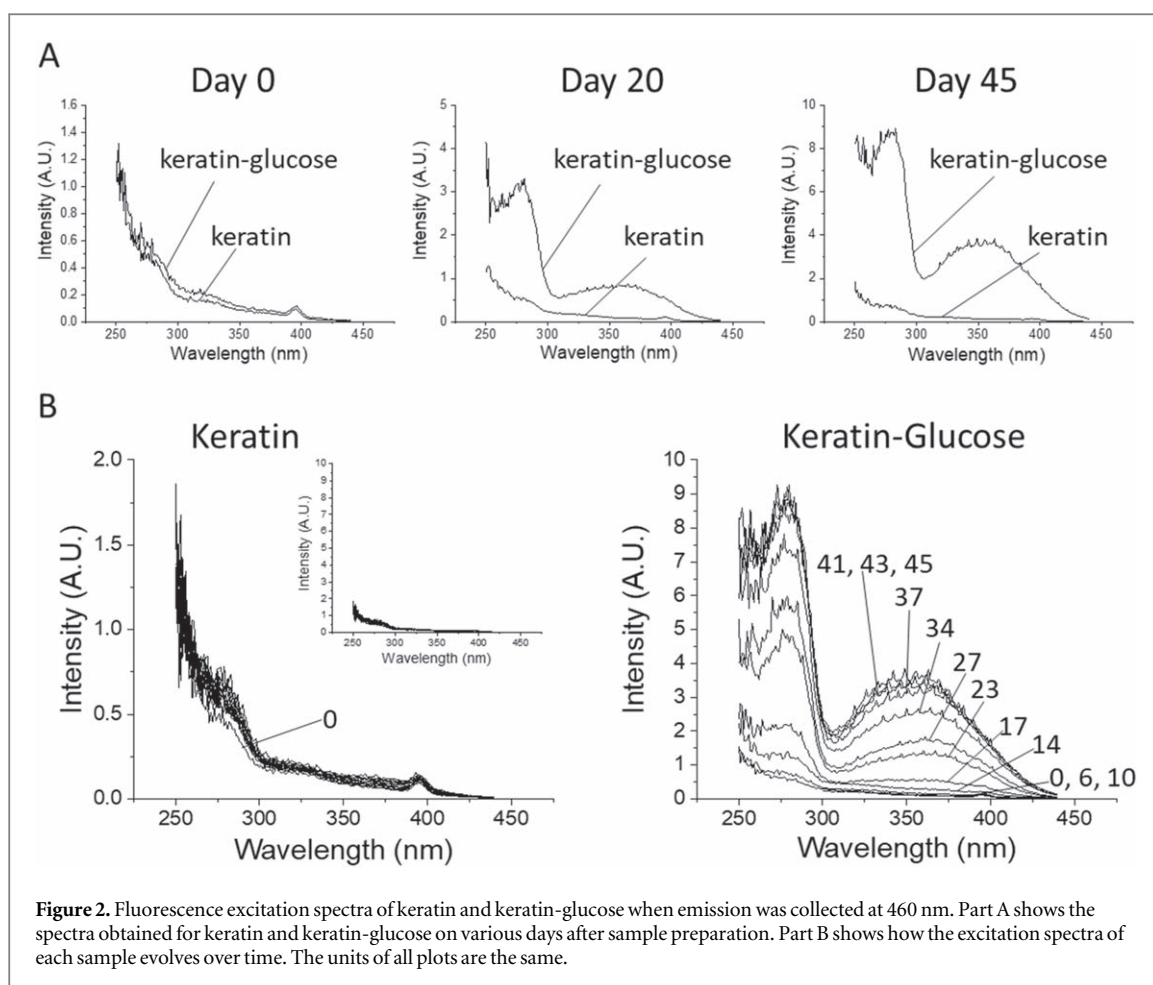
Results and discussion

Figure 1 shows the excitation-emission matrix for keratin and keratin glucose at Day 0 and Day 44. The results at Day 0 are very similar for both samples. The greatest fluorescence intensity occurs for $\lambda_{ex} = 280$ nm, resulting in emission between 300 and 340 nm, corresponding to Tyr and Trp fluorescence in keratin. From the literature [20, 26] there should also be a fluorescence peak between 440 and 460 nm. Indeed, by day 44 there is an increase in fluorescence intensity at this wavelength in both samples, with the intensity substantially greater in the sample with glucose. Hence we have studied in more detail fluorescence of the samples for two excitation wavelengths, 280 nm and 370 nm.

Figure 2 shows the excitation spectra of free keratin and keratin-glucose for the fluorescence associated with cross-links detected at 460 nm. At day 0, the spectra for the two samples are very similar, and the

intensity is at a low level. Over time, the substantial changes can be seen in the keratin-glucose sample (figures 2(A) and (B)). After approximately 10 days, a new broad band appears in the excitation spectra, with a peak wavelength of ~ 370 nm. The fluorescence intensity at this excitation wavelength grows considerably as the keratin-glucose sample evolves, before it stabilises after around 37 days. Absorption at 370 nm is known from literature as a characteristic of keratin cross-links [28]. Thus, we assume that glucose is causing the formation of new cross-links that can be excited directly at 370 nm and emit fluorescence at 460 nm.

Figure 2(B) also shows an increase over time in the 460 nm fluorescence intensity when the keratin-glucose sample is excited at 280 nm. A possibility is that this is fluorescence from kynurenine, which emits weakly at ~ 480 nm when excited at 365 nm [31], which is within the wavelength range considered. Kynurenine is a metabolite of Trp, however its formation requires the presence of certain enzymes [32] (Tryptophan 2,3-dioxygenase (TDO) or Indoleamine 2,3-dioxygenase (IDO)), which are not present in our *in vitro* set up. We therefore hypothesise that the Trp in keratin absorbs the energy at 280 nm, and then



transfers this energy to the keratin cross-links, resulting in increased emission at 460 nm. This transfer of energy could be radiative (re-absorption) or non-radiative (FRET) and intensifies over time as the cross-links are being formed.

The fluorescence spectra in figure 3 show that exciting keratin-glucose sample at 280 nm causes increase in Trp fluorescence at ~ 340 nm when the sample ages. Interestingly excitation at 280 nm also results in fluorescence emission at 460 nm, which correlates to the emission wavelength for keratin cross-links. Again, this seems to suggest that the Trp in keratin transfers its excitation energy to the cross-links, causing emission at 460 nm.

The fact that both Trp and keratin cross-links fluorescence increase suggests an increase in the Trp quantum yield, possibly due to reduced quenching by water as crosslinks shield the Trp sites. Figure 3(C) shows the fluorescence of a reference PBS-glucose sample excited at 280 nm, 42 days after its preparation and storing it in the same conditions as the free keratin and keratin-glucose samples. Negligible emission from this sample demonstrates that there is no detectable bacteria growth in the glucose/buffer environment used in keratin samples.

Using the wavelength 370 nm allowed direct excitation of the cross-links (figure 4). Again, both spectra on day 0 are very similar and contain the peak at 424 nm,

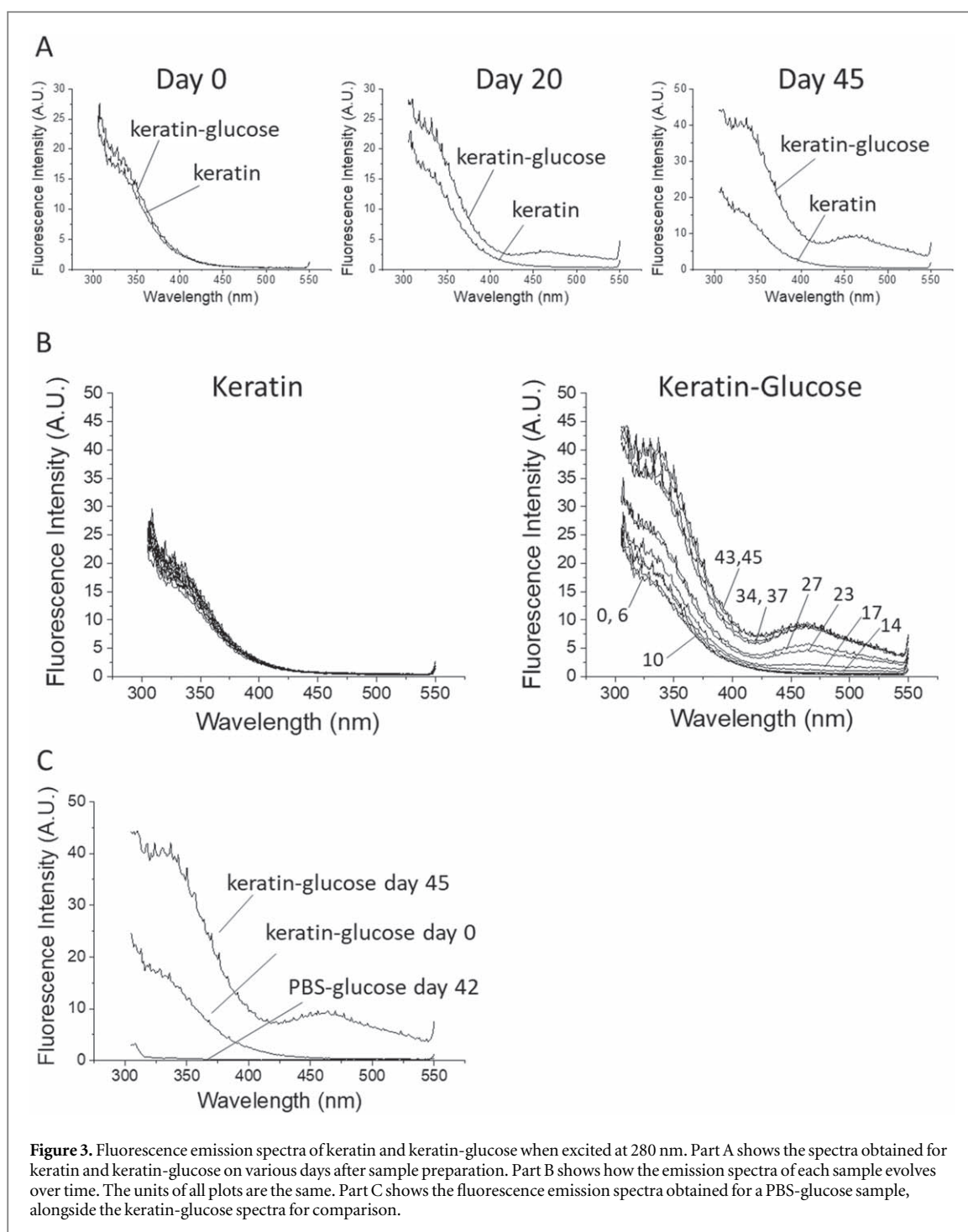
which is the Raman shift for excitation at 370 nm. This was calculated using the Raman shift for water ($3400\text{--}3600\text{ cm}^{-1}$) and the equation

$$\lambda = \frac{1}{1/\lambda_{ex} - \text{Raman shift}/1 \times 10^7} \quad (3)$$

where λ_{ex} is the excitation wavelength used. Both day 0 spectra also show the broad fluorescence band with the peak at ~ 460 nm, associated with the cross-links.

Figure 4(B) shows that in the pure keratin sample the intensity of this fluorescence increases only slightly with time. In the keratin-glucose sample, however, the fluorescence intensity grows substantially as the sample ages, and the dominating peak remains stationary at 460 nm. We also observe the formation of two new peaks at longer wavelengths. After 10 days a second peak starts to appear at ~ 525 nm, and after 21 days, the third peak can be seen at ~ 575 nm. These keratin-glucose complexes form much slower than that responsible for the 460 nm emission and are not observed at all in the free keratin sample.

Similarly like figures 3(C), 4.C also shows that the potential impact of bacteria growth on the keratin and keratin-glucose samples' fluorescence at 370 nm is negligible, and thus any changes observed in the spectra are solely the result of the interaction with glucose and/or protein aggregation.



To quantify the difference in the emission spectra of the two keratin samples for excitation 370 nm, and to illustrate how the spectra evolve over time in more detail, a Gaussian model of fluorescence spectra was fitted to these data.

$$I(\nu) = \sum_{i=1}^M \frac{A_i}{\sigma_i \sqrt{2\pi}} e^{-\left(\frac{\nu - \nu_i}{2\sigma_i}\right)^2} \quad (4)$$

In this model M is the number of spectral components, A_i is the contribution of each component to fluorescence, ν_i is the peak position, and σ_i is the half-width of the distribution. For the pure keratin sample only one component ($M = 1$) was required to describe the

spectra throughout the experiment. This was also adequate for the first 9 days in the keratin-glucose sample; however, 2 components ($M = 2$) were required from day 10, and three components ($M = 3$) were required from day 24. Switching to the more complex model was based on the shape of the spectra and the χ^2 goodness of fit criterion. An additional component represented the Raman scatter at ~ 424 nm. Examples of the experimental fluorescence spectra plotted alongside the model function for keratin and keratin-glucose show relatively good agreement, as can be seen in Supporting Information (SI), Figures S1 and S2.

The evolution of the recovered parameters of the spectra are plotted in figure 5. The initial peak positions

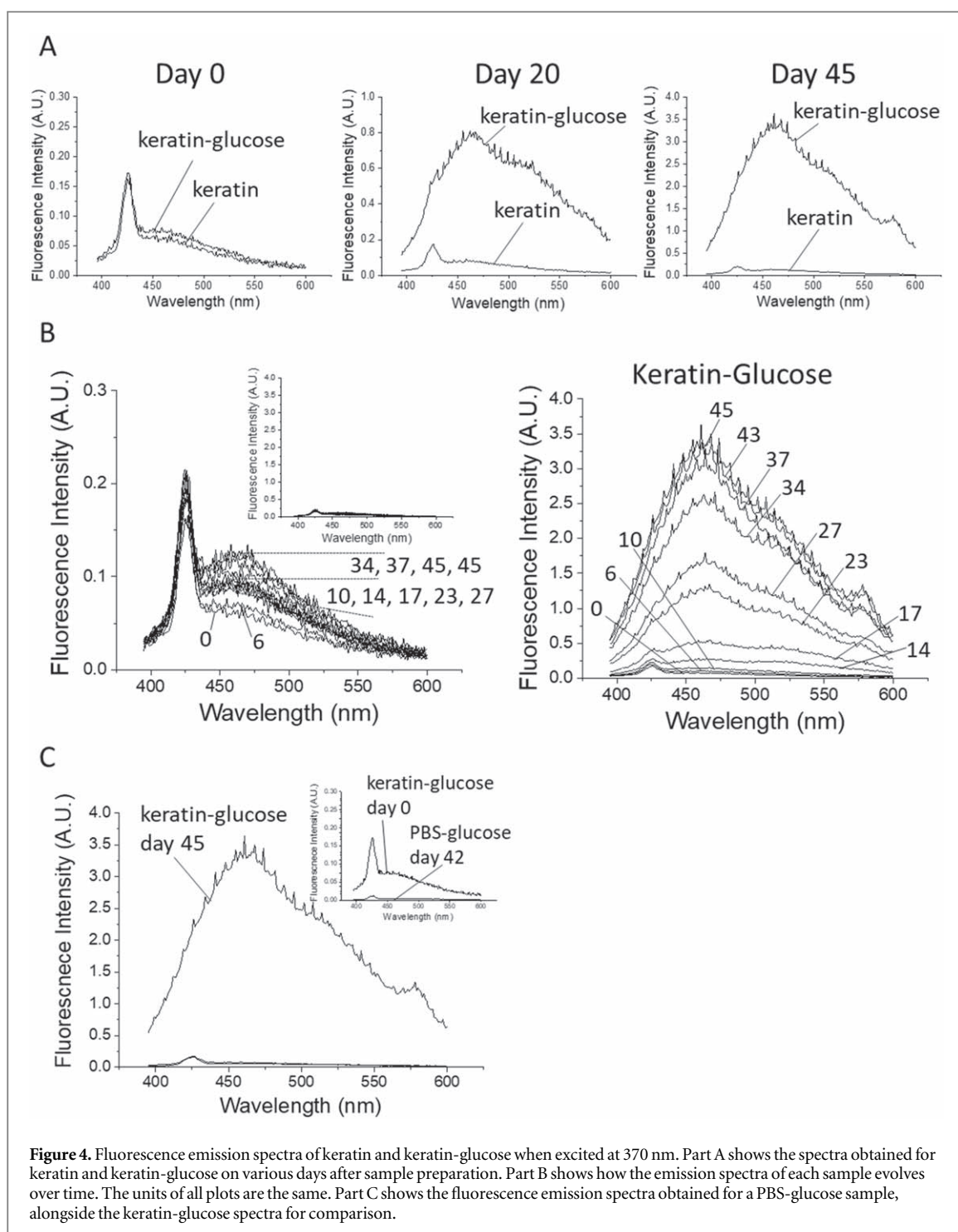
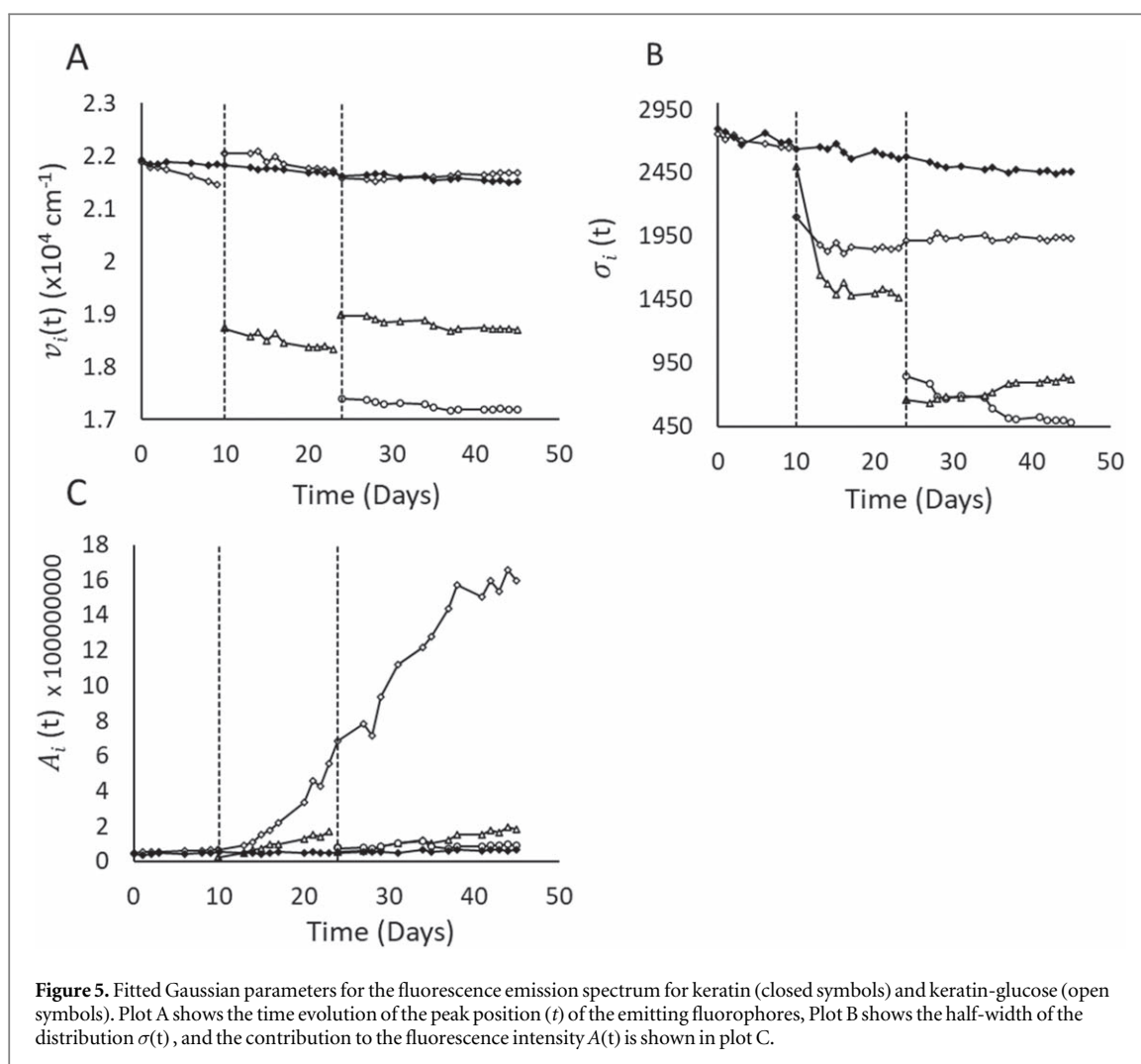


Figure 4. Fluorescence emission spectra of keratin and keratin-glucose when excited at 370 nm. Part A shows the spectra obtained for keratin and keratin-glucose on various days after sample preparation. Part B shows how the emission spectra of each sample evolves over time. The units of all plots are the same. Part C shows the fluorescence emission spectra obtained for a PBS-glucose sample, alongside the keratin-glucose spectra for comparison.

$\nu_1(0)$ for both samples are the same, approximately 22000 cm^{-1} (figure 5(A)), which corresponds to the peak for keratin cross-links. For the pure keratin sample this stays consistent throughout the experiment, but in the keratin-glucose sample, the $\nu_1(t)$ shows a steady decrease through the first 9 days. This drop is likely due to the need for a second component, and indeed when the second component is added to the model, $\nu_1(t)$ increases back to 22000 cm^{-1} , where it remains for the experiment duration. This component is the most dominant contributor to the emission spectrum for both samples, and its contribution $A_1(t)$ increases

substantially in the keratin-glucose sample as the experiment progresses, as illustrated in figure 5(C).

The second component for keratin-glucose also follows the above trend relating to peak position. The $\nu_2(t)$ shows a steady decrease from 18700 cm^{-1} to 18350 cm^{-1} between days 10 and 23, and then once the 3rd component $\nu_3(t)$ is added to the model, $\nu_2(t)$ increases again and remains relatively constant at $\sim 18700\text{ cm}^{-1}$. The peak wavenumber $\nu_3(t)$ for this 3rd component is also stable between day 23 and the experiment end, only showing a slight drop from $\sim 17400\text{ cm}^{-1}$ to $\sim 17200\text{ cm}^{-1}$.



We note that the evolution of the peak wavenumbers $v_i(t)$ is consistent with the evolution of the half-width distributions $\sigma_i(t)$ illustrated in figure 5(B). For free keratin, and for keratin-glucose during the first 10 days, the $\sigma_1(t)$ is large. Although it decreases slightly for the keratin sample over time, there is not a significant change. For keratin glucose, the addition of a second component from day 10 causes the $\sigma_1(t)$ to drop significantly as one component splits into 2, and this happens again at day 24, when the addition of a third component causes $\sigma_2(t)$ to drop as the second component splits again.

This steady state analysis shows how the intrinsic fluorescence of keratin changes in the presence of glucose. The fluorescence of the dominating crosslinks K_{CL} emit at 460 nm and the higher-order crosslinks, K_{CL}' and K_{CL}'' , formed at slower rates, emit at 525 nm and 575 nm, respectively.

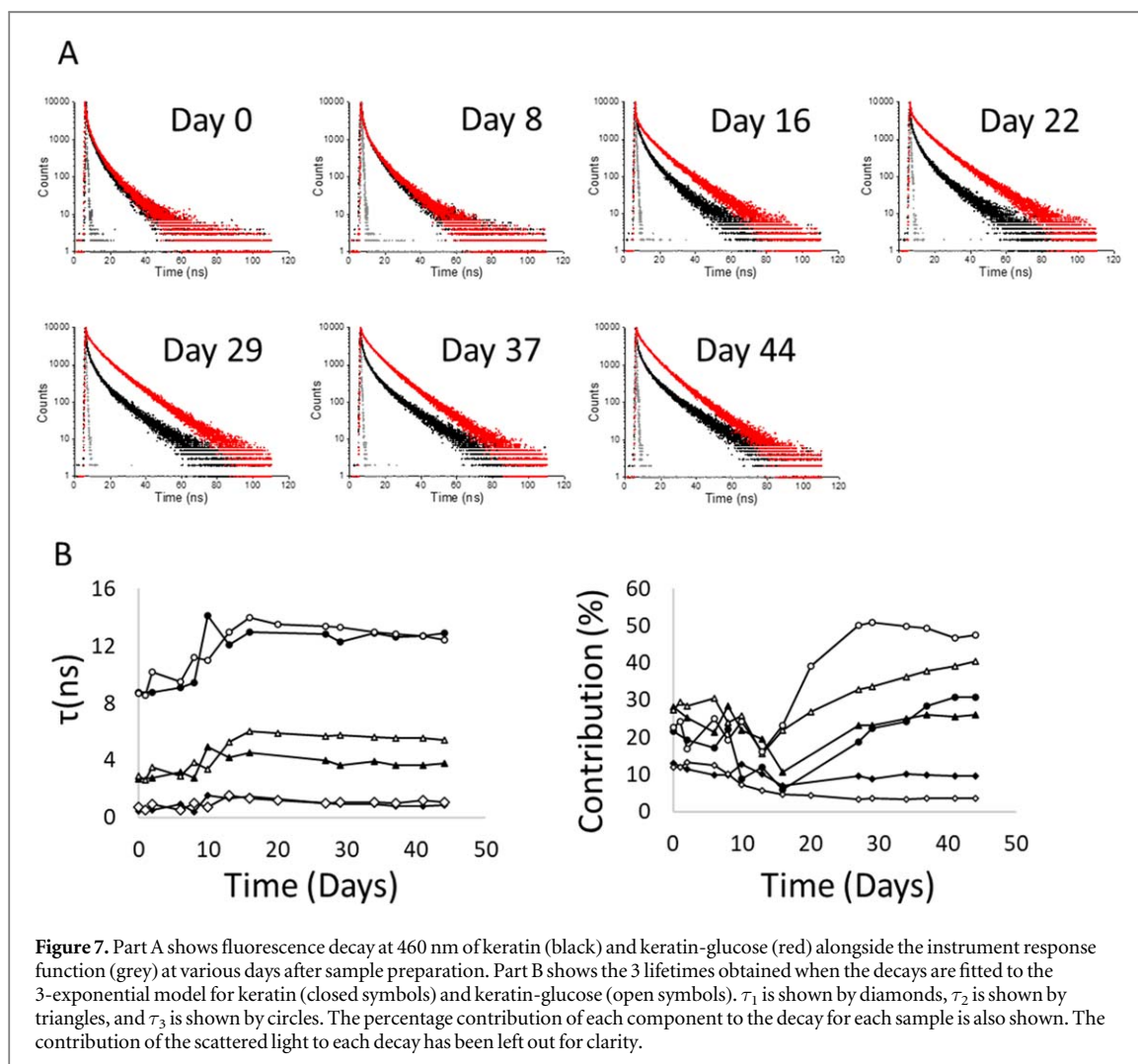
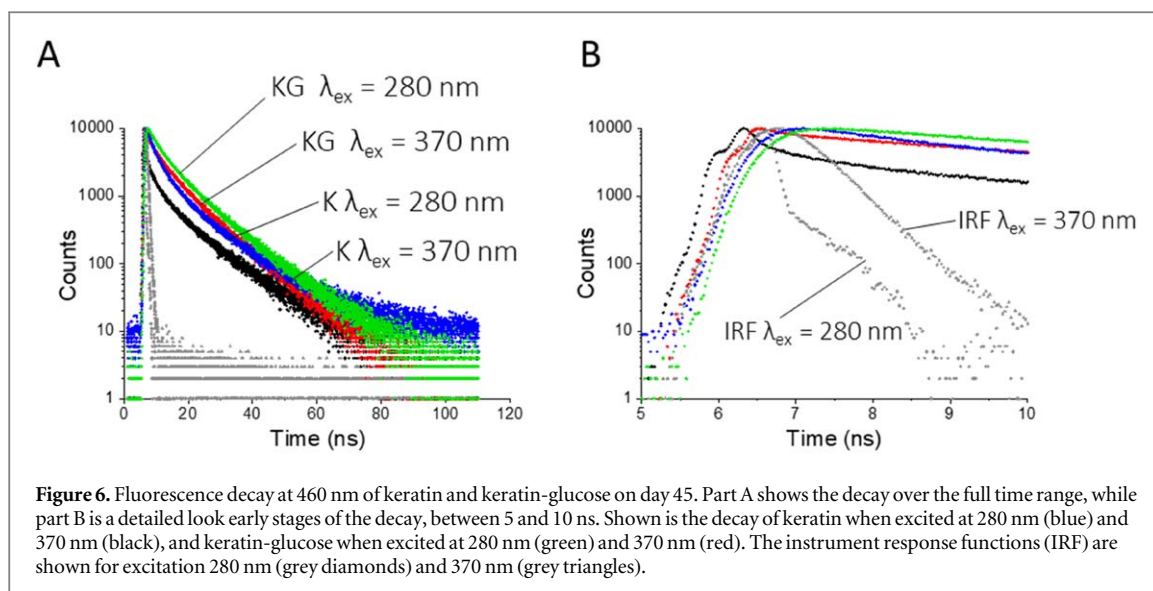
Time resolved measurements were also conducted and analysed for the keratin and keratin-glucose samples. Firstly, the fluorescence intensity decays of both samples at the detection wavelength 460 nm were measured with using two excitation wavelengths 280 nm and 370 nm. The results shown in figure 6 were

carried out at the end of the experiment, on day 45, to maximise the potential impact of glucose.

We note, that for the excitation at 370 nm, the samples begin to decay immediately after excitation (black and red curves). However, for the excitation at 280 nm (blue and green), the top sections of the decays are much flatter, indicating that the detected fluorescence is likely to come from the fluorophore which was not excited directly. Again, these results suggest the transfer of the excitation energy from tryptophan to the cross-links. Moreover, as we observe a substantial spectral overlap between the emission spectrum of the amino acids and the absorption of the cross-links (300–400 nm, seen on the excitation spectra, figure 2), the likely mechanism involved is FRET.

Fluorescence intensity decays at the excitation wavelength of 370 nm and collected at 460 nm at various days following sample preparation are shown in figure 7.

Up to day 8, the raw decays for both samples, with and without glucose, are almost identical (figure 7(A)), however, by day 16, the decays of the glucose-containing sample become slower as compared to those of the pure keratin sample. Figure 7(B) shows the lifetimes and percentage contributions of each component for the data fitted to 3-exponential model decay (see SI for



details). All three lifetimes and their corresponding pre-exponential factors are quite stable and similar between samples during the first ~ 10 days. Between days 10 and 14 the lifetime components show an increase in both samples, and then stabilise for the remainder of the experiment.

Although the three lifetimes appear similar in glucose and glucose-free samples, the impact of glucose manifests itself in changes of the lifetime contributions to the decay. Indeed, the increases in contributions of the two longer lifetime components are much more pronounced in the sample with glucose.

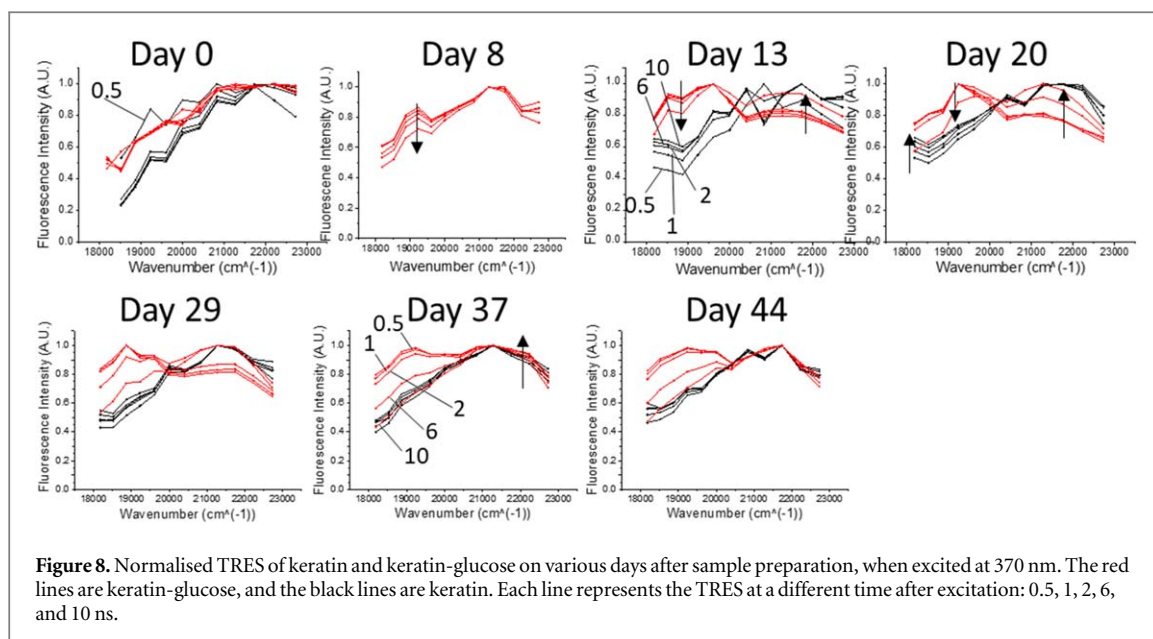


Figure 8. Normalised TRES of keratin and keratin-glucose on various days after sample preparation, when excited at 370 nm. The red lines are keratin-glucose, and the black lines are keratin. Each line represents the TRES at a different time after excitation: 0.5, 1, 2, 6, and 10 ns.

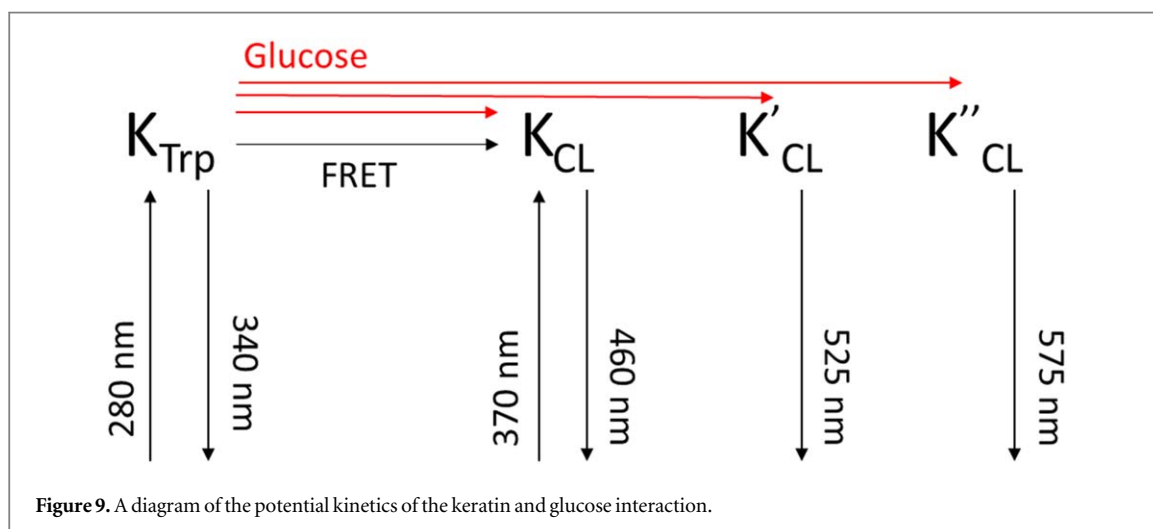


Figure 9. A diagram of the potential kinetics of the keratin and glucose interaction.

Our fitted values do not however seem to be similar to what has been observed in literature. Studies have considered the fluorescence decay of hair, which also contains keratin protein. A 2007 study found a 2-exponential model was sufficient to fit the fluorescence decay of hair, and attributed the long lifetime component of 1.4 ns to keratin [33]. A further study in 2012 found the fluorescence decay of hair to have a more complex multi-exponential decay, and thus used phasor plots to represent it [34]. Our results *in vitro* also appear to show keratin as having a complex multi-exponential decay.

Further information has been gathered from the time-resolved emission spectra (TRES) constructed from the fluorescence intensity decays recorded at a range of wavelengths (440–550 nm) for both samples. Figure 8 shows the normalised TRES for both samples at different times.

The curves for the pure keratin sample (black) do not change shape throughout the decay, indicating

simple fluorescence kinetics. They also do not change substantially during 44 days of the experiment.

Conversely, the shape of the TRES for the keratin-glucose sample does change as the experiment progresses. Initially, at day 0, the TRES resembles the spectrum seen for free keratin, demonstrating no immediate impact of glucose on keratin fluorescence.

By day 13 there seems to be one peak in the TRES, and thus one fluorescent residue, which is consistent with the steady state data. However, after day 13 a second peak can be seen in the TRES, which becomes more pronounced as the experiment progresses. This occurs at 19000 cm^{-1} , and so would correspond to the keratin-glucose complex that forms at approximately 525 nm.

The shape of the spectra also changes in the 10 ns following excitation in the keratin-glucose sample, with the red curves in figure 8 indicating that the fluorescent residue with peak at 525 nm decays faster than the residue at 21500 cm^{-1} ($\sim 460\text{ nm}$). We speculate

that the fluorescence at 525 nm originates from a keratin-glucose complex, which requires a longer time to form, thus it is likely to be a bigger structure than the one emitting at 460 nm, for example one formed by an agglomeration of aggregates rather than by unimolecular addition. The other emission maximum observed at 575 nm may come from even larger keratin-glucose structures. In future studies that the hypothesis of glucose causing the formation of larger complexes, could be confirmed using fluorescence anisotropy measurements.

Conclusion

The data presented have shown that glucose has a big impact on the intrinsic fluorescence of keratin *in vitro*. In pure keratin, fluorescence shows peak at 340 nm due to Trp, and at 460 nm due to cross-links in the protein. These cross-links can be excited directly at 370 nm, or at 280 nm via FRET from the Trp residues. When glucose is added to a keratin sample, the fluorescence intensity at 460 nm increases greatly due to faster formation of new cross-links. Glucose also causes the formation of two new fluorescent complexes with peak fluorescence at ~525 nm (which appears after ~10 days) and 575 nm (~21 days). A schematic diagram illustrating the likely kinetics is shown in figure 9. We anticipate that the contributions of the three compounds detected in this experiment may be different in different conditions of keratin glycation, e.g. in the nail or hair tissues. As keratin intrinsic fluorescence is sensitive to the extent of glucose in its local environment, studying the fluorescence of nail or hair, where keratin is an abundant protein, may offer a complementary method for monitoring long-term complications of diabetes. We are currently exploring further possibilities in this area and the findings will be published in due course.

Acknowledgments

The authors have declared that no conflicting interests exist. RM acknowledges the support of the OPTIMA Doctoral Training Centre.

Data availability statement

The data that support the findings of this study are available upon reasonable request from the authors.

ORCID iDs

Rhona Muir  <https://orcid.org/0000-0002-7851-5659>

David J S Birch  <https://orcid.org/0000-0001-6400-1270>

Olaf J Rolinski  <https://orcid.org/0000-0002-7838-779X>

References

- [1] Nathan D M 2014 The diabetes control and complications trial/epidemiology of diabetes interventions and complications study at 30 years: overview *Diabetes Care* **37** 9–16
- [2] World Health Organisation 2016 *Global Report on Diabetes*
- [3] Singh V P, Bali A, Singh N and Jaggi A S 2014 Advanced glycation end products and diabetic complications *The Korean Journal of Physiology & Pharmacology* **18** 1
- [4] Negre-Salvayre A, Salvayre R, Auge N, Pamplona R and Portero-Otin M 2009 Hyperglycaemia and glycation in diabetic complications *Antioxidants and Redox Signaling* **11** 12
- [5] Reiser K M 1991 Nonenzymatic glycation of collagen in aging and diabetes *Proc. Soc. Exp. Biol. Med.* **196** 17–29 From NLM
- [6] Schneider S L and Kohn R R 1981 Effects of age and diabetes mellitus on the solubility and nonenzymatic glycosylation of human skin collagen *J. Clin. Invest.* **67** 1630–5
- [7] Bourdon E, Loreau N and Blache D 1999 Glucose and free radicals impair the antioxidant properties of serum albumin *FASEB J.* **13** 233–44 From NLM
- [8] Qiu H-Y, Hou N-N, Shi J-F, Liu Y-P, Kan C-X, Han F and Sun X-D 2021 Comprehensive overview of human serum albumin glycation in diabetes mellitus *World Journal of Diabetes* **12** 1057–69
- [9] Nathan D M, Kuenen J, Borg R, Zheng H, Schoenfeld D and Heine R J 2008 Translating the A1C assay into estimated average glucose values *Diabetes Care* **31** 1473–8 From NLM
- [10] Paisey R B, Clamp J R, Kent M J, Light N D, Hopton M and Hartog M 1984 Glycosylation of hair: possible measure of chronic hyperglycaemia *Brit. Med. J.* **288** 669–71
- [11] Bakan E and Bakan N 1985 Glycosylation of nail in diabetics: possible marker of long-term hyperglycemia *Clin. Chim. Acta* **147** 1–5 From NLM
- [12] Delbridge L, Ellis C S, Robertson K and Lequesne L P 1985 Non-enzymatic glycosylation of keratin from the stratum corneum of the diabetic foot *Br. J. Dermatol.* **112** 547–54 From NLM
- [13] Ansari N A, Moinuddin and Ali R 2011 Glycated lysine residues: a marker for non-enzymatic protein glycation in age-related diseases *Dis. Markers* **30** 317–24 From NLM
- [14] Mennella C, Visciano M, Napolitano A, Del Castillo M D and Fogliano V 2006 Glycation of lysine-containing dipeptides *J. Pept. Sci.* **12** 291–6
- [15] Marova I, Zahejsky J and Sehnalova H 1995 Non-enzymatic glycation of epidermal proteins of the stratum corneum in diabetic patients *Acta Diabetologica* **32** 38–43
- [16] Kishabongo A S, Katchunga P, Van Aken E H, Speeckaert R, Lagniau S, Coopman R, Speeckaert M M and Delanghe J R 2015 Glycation of nail proteins: from basic biochemical findings to a representative marker for diabetic glycation-associated target organ damage *PLoS One* **10** e0120112
- [17] Monteyne T et al 2018 Analysis of protein glycation in human fingernail clippings with near-infrared (NIR) spectroscopy as an alternative technique for the diagnosis of diabetes mellitus *Clinical Chemistry and Laboratory Medicine (CCLM)* **56** 1551–8
- [18] Jurgeleviciene I, Stanislovaityene D, Tatarunas V, Jurgelevicius M and Zaliuniene D 2020 Assessment of absorption of glycated nail proteins in patients with diabetes mellitus and diabetic retinopathy *Medicina* **56** 658
- [19] Pena A M, Strupler M, Boulesteix T and Schanne-Klein M C 2005 Spectroscopic analysis of keratin endogenous signal for skin multiphoton microscopy *Opt. Express* **13** 6268
- [20] Voloshina O V, Shirshin E A, Lademann J, Fadeev V V and Darvin M E 2017 Fluorescence detection of protein content in house dust: the possible role of keratin *Indoor Air* **27** 377–85
- [21] Dyer J M, Bringans S D and Bryson W G 2006 Characterisation of photo-oxidation products within photoyellowed wool proteins: tryptophan and tyrosine derived chromophores *Photochemical & Photobiological Sciences* **5** 698
- [22] Block R J 1939 The composition of keratins *J. Biol. Chem.* **128** 181–6

- [23] Ghisaidoobe A and Chung S 2014 Intrinsic tryptophan fluorescence in the detection and analysis of proteins: a focus on Förster resonance energy transfer techniques *Int. J. Mol. Sci.* **15** 22518–38
- [24] Lakowicz J R 2006 *Principles of Fluorescence Spectroscopy* (Berlin: Springer)
- [25] Chen Y and Barkley M D 1998 Toward understanding tryptophan fluorescence in proteins *Biochemistry* **37** 9976–82 From NLM
- [26] McMullen R L, Chen S and Moore D J 2012 Spectrofluorescence of skin and hair *Int. J. Cosmet. Sci.* **34** 246–56
- [27] Strnad P, Usachov V, Debes C, Gräter F, Parry D A D and Omary M B 2011 Unique amino acid signatures that are evolutionarily conserved distinguish simple-type, epidermal and hair keratins *J. Cell Sci.* **124** 4221–32
- [28] Kollias N, Zonios G and Stamatas G N 2002 Fluorescence spectroscopy of skin *Vib. Spectrosc.* **28** 17–23
- [29] Na R, Stender I M, Henriksen M and Wulf H C 2001 Autofluorescence of human skin is age-related after correction for skin pigmentation and redness *J Invest Dermatol* **116** 536–40 From NLM
- [30] Rolinski O J, Wellbrock T, Birch D J S and Vyshemirsky V 2015 Tyrosine photophysics during the early stages of β -amyloid aggregation leading to Alzheimer's *The Journal of Physical Chemistry Letters* **6** 3116–20
- [31] Fukunaga Y, Katsuragi Y, Izumi T and Sakiyama F 1982 Fluorescence characteristics of kynurenine and N¹-formylkynurenine, their use as reporters of the environment of tryptophan 62 in hen egg-white lysozyme I *The Journal of Biochemistry* **92** 129–41
- [32] Davis I and Liu A 2015 What is the tryptophan kynurenine pathway and why is it important to neurotherapeutics *Expert Review of Neurotherapeutics* **15** 719–21
- [33] Ehlers A, Riemann I, Stark M and König K 2007 Multiphoton fluorescence lifetime imaging of human hair *Microsc. Res. Tech.* **70** 154–61
- [34] Krasieva T B, Stringari C, Liu F, Sun C-H, Kong Y, Balu M, Meyskens F L, Gratton E and Tromberg B J 2012 Two-photon excited fluorescence lifetime imaging and spectroscopy of melanins *in vitro* and *in vivo* *J. Biomed. Opt.* **18** 031107